ORIGINAL ARTICLE

JKMS

http://dx.doi.org/10.3346/jkms.2014.29.S3.S237 • J Korean Med Sci 2014; 29: S237-248

Effect of Endogenous Bone Marrow Derived Stem Cells Induced by AMD-3100 on Expanded Ischemic Flap

Hii-Sun Jeong,[1,2] Hye-Kyung Lee,[3] Kwan-Chul Tark,[2] Dae-Hyun Lew,[2] Yoon-Woo Koh,[4] Chul-Hoon Kim,[5] and In-Suck Seo[1]

[1]Department of Plastic & Reconstructive Surgery, Kangnam Sacred Heart Hospital, Hallym University Medical Center, Halllym University College of Medicine, Seoul; [2]Department of Plastic and Reconstructive Surgery, Institute for Human Tissue Restoration, Yonsei University College of Medicine, Seoul; [3]Department of Plastic and Reconstructive Surgery, Eulji General Hospital, Eulji University School of Medicine, Seoul; Departments of [4]Otorhinolaryngology, [5]Pharmacology, Yonsei University College of Medicine, Seoul, Korea

Received: 6 June 2014
Accepted: 17 September 2014

Address for Correspondence:
Hii-Sun Jeong, MD
Department of Plastic and Reconstructive Surgery, Kangnam Sacred Heart Hospital, Hallym University Medical Center, Hallym University College of Medicine, 1 Singil-ro, Yeongdeungpo-gu, Seoul 150-950, Korea
Tel: +82.2-829-5182, Fax: +82.2-847-5183
E-mail: hiisunj@gmail.com

The purpose of this study was to devise an expanded ischemic flap model and to investigate the role of AMD-3100 (Plerixafor, chemokine receptor 4 inhibitor) in this model by confirming its effect on mobilization of stem cells from the bone marrow. Male Sprague-Dawley rats were used as an animal research model. The mobilization of stem cells from the bone marrow was confirmed in the AMD-3100-treated group. The fractions of endothelial progenitor cells (EPC) and the vascular endothelial growth factor receptor (VEGFR) 2+ cells in the peripheral blood were increased in groups treated with AMD-3100. The expression of vascular endothelial growth factor (VEGF) was increased in response to expansion or AMD injection. The expression of stromal cell derived factor (SDF)-1 and VEGFR2 were increased only in unexpanded flap treated with AMD-3100. Treatment with AMD-3100 increased both the number and area of blood vessels. However, there were no statistically significant differences in the survival area or physiologic microcirculation in rats from the other groups. This endogenous neovascularization induced by AMD-3100 may be a result of the increase in both the area and number of vessels, as well as paracrine augmentation of the expression of VEGF and EPCs. However, the presence of a tissue expander under the flap could block the neovascularization between the flap and the recipient regardless of AMD-3100 treatment and expansion.

Keywords: Endothelial Progenitor Cell; Hematopoietic Stem Cell; Tissue Expansion; Ischemic Flap; AMD-3100; CXCR4 Inhibitor; Plerixafor

INTRODUCTION

Tissue expansion of the skin and soft tissue adjacent to cover the defect provides advantages such as identical skin color, texture and skin appendage to that of the defect.

This method reduces donor site morbidity and provides good cosmetic results. In cases of scanty donor tissue or the possibility of growth of children (such as separation of conjoined twins or removal of congenital giant nevus) tissue expansion is necessary and appropriate as a reconstruction modality (1-3).

The region under tissue expansion has a favorable microenvironment for tissue regeneration (4). Expression of growth factors such as VEGF, PDGF, and EGF is increased in environments that require tissue regeneration. VEGF expression is significantly greater around the tissue expander, as compared with the original flap, as a result of continued VEGF expression under the conditions of constant low partial pressure of oxygen (5-7). Tissue expansion takes place due to increased cell proliferation following activation of protein kinase leading to intracellular signal transduction (8).

Stem cells migrate from the bone marrow to the peripheral blood, differentiate into endothelial progenitor cells (EPCs), and proliferate as EPCs (9-11). The microenvironment that produces growth factors such as VEGF, PDGF, and EGF can be likened to soil, and the EPCs can be likened to seeds planted in this soil (12). In order to improve the survival rate of the expanded flap, there should be an increase in angiogenesis and vasculogenesis, which requires a favorable microenvironment with over-expression of VEGF and mobilization of greater numbers of precursor cells such as EPCs.

C-X-C chemokine receptor type 4 (CXCR4) is a cell surface receptor on bone marrow hematopoietic stem cells. CXCR4 binds to stromal cell-derived factor 1 (SDF-1) in the bone marrow, promoting homing of hematopoietic stem cells to the bone marrow (13). AMD-3100 is now clinically used with pretreated granulocyte colony-stimulating factor (G-CSF) to promote mobilization of hematopoietic stem cells to the peripheral blood in patients with non-Hodgkin's lymphoma or multiple myeloma

pISSN 1011-8934
eISSN 1598-6357

who require stem cell auto transplantation (14). When AMD-3100 is pre-treated with VEGF, this inhibits binding between CXCR4 on hematopoietic stem cells and SDF-1 in the bone marrow. By facilitating mobilization and differentiation of hematopoietic stem cells, the number of EPCs and mesenchymal cells in the peripheral blood rises by one hundredfold (15).

If treatment with AMD-3100 increases mobilization of EPCs in expanded flap tissues, it is possible that a smaller harvested donor flap could reconstruct a larger defect after expansion and therefore reduce donor site morbidity. It may also make it possible to reduce patient discomfort by reducing expansion time. Finally, the survival of expanded flaps may be improved by treatment with AMD-3100 by promoting vasculogenesis through expression of VEGF and mobilization of EPCs.

The purpose of this study was to devise an expanded ischemic flap model and to investigate the role of AMD-3100 in expanded ischemic flaps by demonstrating its effect on mobilization of EPCs from the bone marrow.

MATERIALS AND METHODS

Animals

The study utilized male Sprague-Dawley rats (body weight, 300-400 g). All animal procedures were carried out according to a protocol approved by the institutional animal care and use committee in Yonsei University (IACUC approval No. 2011-0026). Isoflurane (Aerane®, Ilsung Pharmaceuticals, Seoul, Korea) was used as an inhalation anesthetic. Zolazepam-tiletamine mixture (30 mg/kg, Zoletil®, Virbac, Carrs, France) and xylazine (10 mg/kg, Rumpun®, Bayer, Seoul, Korea) were administered as needed, by intraperitoneal injection.

Classification of experimental and control groups by administration of AMD-3100 and procedure

Classical dorsal axial patterned flaps (3 × 9 cm) were prepared on the backs of 42 rats without insertion of silicone to conduct the Preliminary study for determination of optimal dosage and route of administration for AMD-3100. After preparation of skin flaps, groups of rats were divided by dosage of AMD-3100 (5 or 10 mg/kg) and injection route (subcutaneous, intravenous or intraperitoneal) (n = 7 rats per group). Following injection of AMD-3100, vasculogenesis and angiogenesis were measured by the survival area and photographically analyzed using Image J® software (NIH-Scion Corporation, Bethesda, MD, USA).

A total of 28 rats were divided into four groups (n = 7 rats per group) for the preliminary study on the effect of AMD-3100 and insertion of silicone sheets to block neovascularization from the bed of a classical unexpanded flap. Classical caudal based axial patterned dorsal skin flaps (3 × 9 cm) were elevated for all rats. A silicone sheet were placed between the elevated flap and the bed in groups B and D, but not in groups A and C. AMD-3100 was injected into rats in groups C and D in accordance with the optimal dosage and route determined above (Table 1). AMD-3100 was not administered to rats in groups A and B, and instead an equivalent amount of phosphate-buffered saline (PBS) was administered.

Main study was proceeded to investigate the effects of treatment with AMD-3100 in the expanded flap model. A total of 40 rats were divided into four groups (n = 10 rats per group) as listed in Table 2: Group I (control group, skin random pattern flap [3 × 9 cm], elevation without AMD-3100 injection), Group II (flap expansion, without AMD-3100 injection), Group III (flap elevation and treatment with AMD-3100 injection), and Group IV (flap expansion and treatment with AMD-3100 injection). Rats that did not receive AMD-3100 were injected with an equivalent volume of PBS.

Injection protocol for AMD-3100 (EPC modulator, Mozobil®)

Thirty minutes, 24 hr, and 48 hr after flap elevation, the 10 mg/kg of AMD-3100 (Sigma, St Louis, MO, USA) was injected subcutaneously at the mid-point between the scapulae, 2 cm away from the distal portion of the flap. This dosage and route of administration were determined to be optimal in the preliminary experiments.

Expanded skin flap animal model

The design for tissue expansion of ischemic skin flaps is as shown in Fig. 1. A flap based on the tail measuring 3.0 × 9.0 cm was elevated on the back of each rat. The proximal portion of the flap was created at the ischial protuberance, and a 1.0 cm area from the distal edge of the flap was removed for replacement by the expanded skin flap. The flap consisted of 3 layers (skin, panniculus carnosus, and submuscular connective tissue), and did not include axial vessels. The edge of expanded skin flap was repaired with #4-0 nylon continuous suture technique by including bed, silicone sheet and donor site to maintain the expansion and prevent vessel embedding between the flap and recipient site. In order to block blood flow from the floor, a 5 × 10 cm sized silicone sheet (0.13 mm thick, 4 × 11 cm, Bioplexus

Table 1. Classification of groups of rats in the preliminary study

Group	Group A	Group B	Group C	Group D
AMD-3100	- (PBS)	- (PBS)	+	+
Silicone sheet	-	+	-	+

PBS, Phosphate buffered solution.

Table 2. Classification of main study group

Group	Group I (control)	Group II	Group III	Group IV
AMD-3100	- (PBS)	- (PBS)	+	+
Expansion	-	+	-	+

PBS, Phosphate buffered solution.

http://dx.doi.org/10.3346/jkms.2014.29.S3.S237

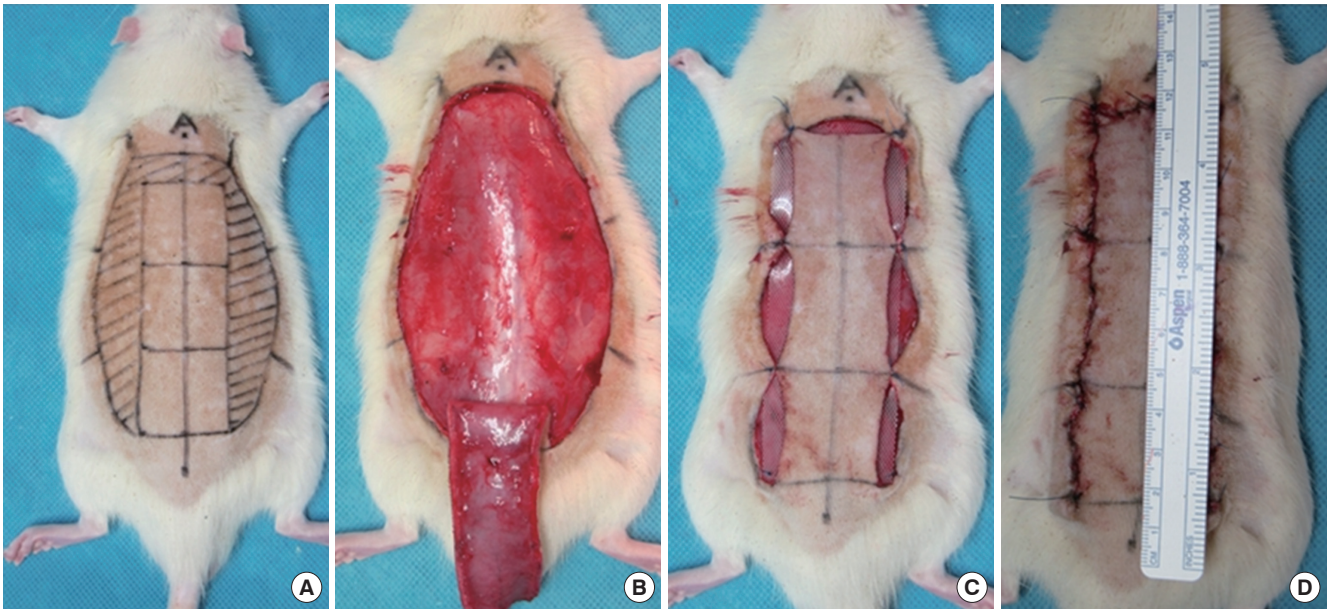

Fig. 1. Expanded skin flap animal model. (**A**) Design of expanded ischemic random pattern skin flap. (**B**) Edge of the distal flap removed for skin expansion. Flap elevation above the submuscular connective tissue. (**C**) Silicone placement on the floor. (**D**) Final suture state.

Corporation®, CA, USA) was placed under the flap and routine dressing was not enforced.

Differentiation and mobilization of EPCs from bone marrow hematopoietic stem cells following injection of AMD-3100

After collection of whole blood at 24 and 48 hr postoperatively, we harvested bone marrow from the femurs of four rats from each group. After shaving and sterilization with alcohol and povidone, both right and left femurs and tibias were obtained from rats at postoperative day 2 to harvest bone marrow. Bone marrow was harvested from both articular areas by washing with sterile PBS using a 5 mL syringe. The collected solution was centrifuged (150 g, 10 min), and the supernatant was immediately stored at -70°C.

To measure active MMP-9, gelatin zymography was used. The concentration of protein in each bone marrow sample was quantified using the Bradford Method protein assay kit (Bio-Rad Laboratories, Hercules, CA, USA), which is based on a bovine gamma globulin standard.

Each sample was separated by electrophoresis on 10% polyacrylamide gel containing 0.1% gelatin. The gels were washed with renaturing buffer (25% Triton X-100 solution) for 30 min at room temperature, followed by incubation in activation buffer for 30 min and an additional incubation in fresh developing buffer for 15 hr at 37°C. Following incubation, the gels were stained for 1 hr in a solution of 2% brilliant blue, 50% ethanol and 10% acetic acid. After bleaching for 30 min in 30% methanol mixed with 10% acetic acid, the gels were fixed in distilled water. The density of each lytic band was measured using a 2020 Ultrascan Laser Densitometer (LKB, Sweden).

To characterize the phenotypes of bone marrow derived stem cell in peripheral blood, flow cytometric analysis was performed. Whole blood was collected at 24 hr and 48 hr postoperatively and treated with 0.05% trypsin and 0.53 mM ethylenediamine tetraacetic acid (EDTA) and washed twice with PBS. Cell aliquots (1×10^6 cells/mL of PBS) were stained with primary antibodies at room temperature for 30 min.

The primary antibodies were fluorescein isothiocyanate-conjugated anti- CD34 (#7324, Santa Cruz, CA, USA), VEGFR2 (ab 2349, Abcam, Cambridge, Mass., USA), and CD133 (MAB4310, Chemicon, Temecula, CA, USA). Flow cytometry was performed on a fluorescence-activated cell sorter (FACS Calibur, BD Biosciences), and data analysis was performed using Cell Quest software (BD Biosciences).

Measurement of survival area of flaps and blood flow

Flap survival area was measured using digital photo analysis. The colors of digital images obtained at a constant exposure and distance were converted into numerical values. Survival area was defined as the difference between the total area and the demarcated area of necrosis. Survival rate was defined as a percentage by dividing the survival area by the total area. At postoperative day 7, the survival areas over time were compared quantitatively by comparing the digital images obtained from experimental and control groups. The length of each image was converted into the actual length utilizing ImageJ® software (NIH-Scion Corporation, Bethesda, MD, USA).

Laser Doppler was used to assess the physiologic result. At postoperative day 7, laser Doppler (Periflux system 5000®, Perimed

AB, Jarfalla, Sweden) located 2 cm proximal to the base of the flap was used to investigate the variation of blood flow. Rats were anesthetized with with zolazepam-tiletamine mixture (Zoletil®, Virbac, Carrs, France) and an average value for blood flow was calculated from three measurements per rat and recorded as perfusion unit. By placing a probe perpendicular to the flap, it is monitored continuously for 10 sec during each measurement.

Histology for quantitative measurement of vascularization and measuring expressions of VEGF, SDF-1, and HIF-1α in tissue

Seven days after flap elevation, segments of tissue (0.5 × 1.0 cm) were obtained from an area 3 cm away from the base of the flap along the long axis. The skin tissue was embedded in paraffin and 5 μm sections were obtained. Both hematoxylin and eosin staining and immunohistochemical staining for CD31 (anti-CD31 antibody, #1506, Santa Cruz, CA, USA) were performed. Capillaries were observed as a single layer of flattened endothelial cells without smooth muscle, as observed at 200X on an optical microscope (Olympus, Tokyo, Japan). To eliminate bias, capillaries were counted in eight areas (0.46 mm^2) by an independent researcher blinded to the treatment group, and the capillary density was recorded as capillary count/mm^2.

Both hematoxylin and eosin staining and immunohistochemical staining for VEGF (anti-VEGF, #7269, Santa Cruz, CA, USA), SDF-1 (anti-SDF1, #3740S, CST, Danvers, MA, USA) and HIF-1α (anti-HIF-1α, #53546, Santa Cruz, CA, USA) were performed on flap tissue. Expression levels of VEGF, SDF-1 and HIF-1α were analyzed by immunohistochemistry using imaging analysis software (Metamorph®, Universal Imaging Corporation, Downingtown, PA, USA).

Western blot analysis

Western blotting was used to analyze factors that play key roles in vasculogenesis and angiogenesis, including VEGF (anti-VEGF, #7269, Santa Cruz, CA, USA), HIF-1α (anti- HIF-1α, #53546, Santa Cruz, CA, USA) and SDF-1 (anti-SDF-1, #3740S, CST, Danvers, MA, USA). At 7 days after flap elevation, segments of tissue (0.5 ×1.0 cm) were obtained from an area 3cm away from the flap base along the long axis. Tissues were washed with PBS and centrifuged at 3,000 rpm for 2 min, dissolved in RIPA buffer (10 mM PBS, 1% NP40, 0.5% sodium deoxycholate and 0.1% SDS) containing proteinase inhibitors (10 mg/mL PMSF, 30 mg/mL aprotonin [cat #A6279, Sigma, St. Louis, MO, USA], and 10 mg/mL sodium orthovanadate [100 mM]). The obtained samples were treated with electrophoresis loading buffer (1.0 mL glycerol, 0.5 mL 2-mercaptoethanol, 3.0 mL 10% SDS, 1.25 mL 1.0M Tris-HCL [pH 6.7], 1-2 mg bromophenol blue) and simmered for 3 min. 10% SDS-PAGE electrophoresis was performed on nitrocellulose membranes (Millipore Co., Bedford, MA, USA). Membranes were blocked with 10mM Tris-buffered saline (TBS, pH 8.0) containing 5% nonfat dry milk at 4°C overnight. It was treated with anti-rabbit as 1:1,000 diluted secondary antibody and anti-goat (Amersham, Arlington Heights, IL, UK) for 1 hr. Then, membranes were detected radiographically using Amersham Hyperfilm ECL (Amersham, Arlington Heights, IL, UK). Chromophores from the ECL system (Amersham, UK) VEGF concentrations were normalized by β-actin. Concentrations of SDF-1 and HIF1-α were normalized by glyceraldehyde-3-phosphate dehydrogenase (GADPH). Relative protein expression was determined using Image J® software (NIH-Scion Corporation, Bethesda, MD, USA).

Quantitative real-time reverse transcriptase polymerase chain reaction (RT-PCR)

We used RT-PCR to analyze the experimental genes for vascular endothelial growth factor A (VEGFA), vascular endothelial growth factor Receptor 2 (VEGFR2, Flk-1/KDR), endothelial nitric oxide synthase 3 (NOS3, eNOS), stromal cell-derived factor 1α (SDF-1, CXCL12) and hypoxia-inducible factor-1 (HIF-1α). Total RNA was prepared with TRIzol™ Reagent (Invitrogen, Carlsbad, CA, USA), and complementary DNA was prepared from 0.5 μg of total RNA by random priming using a first-strand cDNA synthesis kit (Promega, Fitchburg, WI, USA), under the following conditions: 95°C for 5 min, 37°C for 2 hr, and 75°C for 15 min.

Quantification of mRNA was performed using SYBR green on cycler. TaqMan® primer/probe kits were used to analyze mRNA expression levels by use of an ABI Prism 7500 HT Sequence Detection System (Applied Biosystems, Foster City, CA, USA). Target mRNA levels were measured relative to an internal mouse beta actin (ACTB) control. For cDNA amplification, AmpliTaq Gold® DNA polymerase was activated by incubating for 10 min at 95°C; this was followed by 40 cycles of 95°C for 15 sec and 60°C for one minute per cycle. To measure cDNA levels, the threshold cycle at which fluorescence was first detected above baseline was used, and a standard curve was drawn between the starting nucleic acid concentrations and the threshold cycle. The mRNA expression levels were normalized to the levels of ACTB, and then relative quantification was expressed as fold-induction compared with control conditions (group I). The relative mRNA expression levels were calculated according to the comparative Ct (ΔΔCt) method (Applied Biosystems) (16). The target quantity was normalized to an endogenous control and relative to a calibrator, and was calculated using formal: target amount = $2^{-\Delta\Delta Ct}$.

Statistical analysis

All data obtained were analyzed with SPSS version 18.0 statistical software (SPSS, Inc., Chicago, IL, USA) and verification was performed by the Kruskal-Wallis test and the Mann-Whitney test. Tests were significant at $P < 0.05$.

http://dx.doi.org/10.3346/jkms.2014.29.S3.S237

RESULTS

Selection of the optimal dosage and injection route for AMD-3100

The flap survival rate was highest (93.9%) for subcutaneous injection of 10 mg/kg AMD-3100. ($P < 0.001$, Kruskal-Wallis test; Table 3).

Differentiation and mobilization of EPC from bone marrow hematopoietic stem cells following injection of AMD-3100

As shown by zymography, there were significantly higher levels of active MMP-9 in bone marrow from rats injected with AMD-3100 (groups III and IV) as compared to rats injected with PBS (groups I and II) at postoperative day 2 ($P = 0.045$, Mann-Whitney test).

The fraction of VEGFR2+ cells in the peripheral blood of rats in Group III was significantly higher than any other group on days 1 and 2 after the procedure ($P < 0.001$, Kruskal-Wallis test). On the same days, the fraction of VEGFR2+/CD34+ double-positive cells(EPC) in the peripheral blood of rats from group IV (AMD-3100, expanded) was statistically significantly higher than any other group. ($P < 0.001$, Kruskal-Wallis test) Flow cytometric analysis showed that there were few CD133 positive cells in peripheral blood of all groups, regardless of treatment with AMD 3100.

Survival area of flaps

In rats treated with AMD-3100 and without a silicone sheet, the median survival rate of classical unexpanded flaps (group C) was 94%. This was significantly different from the survival rate of flaps in control rats (group A, no AMD-3100 treatment, no silicone sheet) at postoperative day 7 ($P = 0.004$, Mann-Whitney test; Fig. 2A and Table 4). When a silicone sheet was added, the median survival rate was also significantly higher in rats treated with AMD-3100 (group B) than in rats without treatment (group B vs. group D, $P = 0.002$; Fig. 2B). Insertion of a silicone sheet under the flap significantly decreased the median survival rate compared with flaps in without the silicone sheet (P for group A and B = 0.011, P for group C and D = 0.017), regardless of injection of AMD 3100 (Fig. 2C).

The survival rates (%, median) of flaps with a silicone sheet for group I, group II, group III and group IV were 59%, 50%, 61% and 51.5%, respectively, at postoperative day 7. However, the survival rate of flaps in group I (untreated, unexpanded) was not significantly different from the other groups ($P = 0.068$, Kruskal-Wallis test, Table 5).

The survival rate of flaps in rats treated with AMD-3100 (group III and IV) was not significantly different than of flaps in untreated rats (group I and II, $P = 0.443$, Mann-Whitney test). The survival rate (%, median) of unexpanded flaps (groups I and III) was significantly higher than the survival rate of expanded flaps (group II and IV, $P = 0.004$, Mann-Whitney test). However, the survival rate of flaps for group III (treated with AMD-3100, unexpanded) was significantly higher than that for group IV (treated with AMD-3100, expanded, $P = 0.0029$, Mann-Whitney test).

Table 3. Survival rate of flaps according to injection route of AMD-3100

Groups	Median rate (%) (min-max)	*P* value
5 mg/kg SC	85.2 (78.6-89.5)	< 0.001*
5 mg/kg IV	71.3 (65.9-76.2)	
5 mg/kg IP	81.3 (76.8-86.6)	
10 mg/kg SC	93.9 (89.6-95.3)	< 0.001*
10 mg/kg IV	74.0 (71.2-79.6)	
10 mg/kg IP	89.2 (87.5-93.2)	

*$P < 0.05$, Kruskal-Wallis test. SC, subcutaneous; IV, intravenous; IP, intraperitoneal.

Physiologic assessment of blood flow by laser doppler

At postoperative day 7, blood flow measured by laser Doppler in the proximal portion of the flaps was not significantly different between the groups ($P = 0.534$, Kruskal-Wallis test).

Histology for quantitative measurement of vascularization and measuring expressions of VEGF, SDF-1, and HIF-1α in tissue

At postoperative day 7, groups III and IV (treated with AMD-3100) showed a statistically significant increase in vessel area compared with groups I and II (untreated) ($P < 0.001$, Mann-Whitney test), (Fig. 3). However, there was no significant difference in the area of vessels between groups I and II or between groups III and IV ($P = 0.244$, $P = 0.326$, Mann Whitney test). In the same manner, group III and IV showed a statistically significant increase in vessel number compared with groups I and II ($P < 0.001$, Mann Whitney test). However, there was no significant difference in the area of vessels between groups I and II or between group III and IV ($P = 0.110$, $P = 0.324$, Mann-Whitney test).

At postoperative day 7, the density of VEGF in the proximal portion of the flaps, as measured by immunohistochemistry and Metamorph® software, was significantly different between the groups. Groups II, III and IV showed a significant increase in expression of VEGF compared with group I ($P < 0.001$, Mann-Whitney test; Fig. 4). At postoperative day 7, the density of SDF-1 and HIF-1α in the proximal portion of the flaps, as measured by immunohistochemical staining and Metamorph® software, was not significantly different between the groups ($P = 0.898$, $P = 0.325$, Kruskal-Wallis test).

Western blot analysis

At postoperative day 7, western blot analysis of VEGF, SDF-1 and HIF-1α in the proximal portion of the flaps showed no significant differences between groups ($P = 0.064$, 0.514, and 0.293, Kruskal-Wallis test).

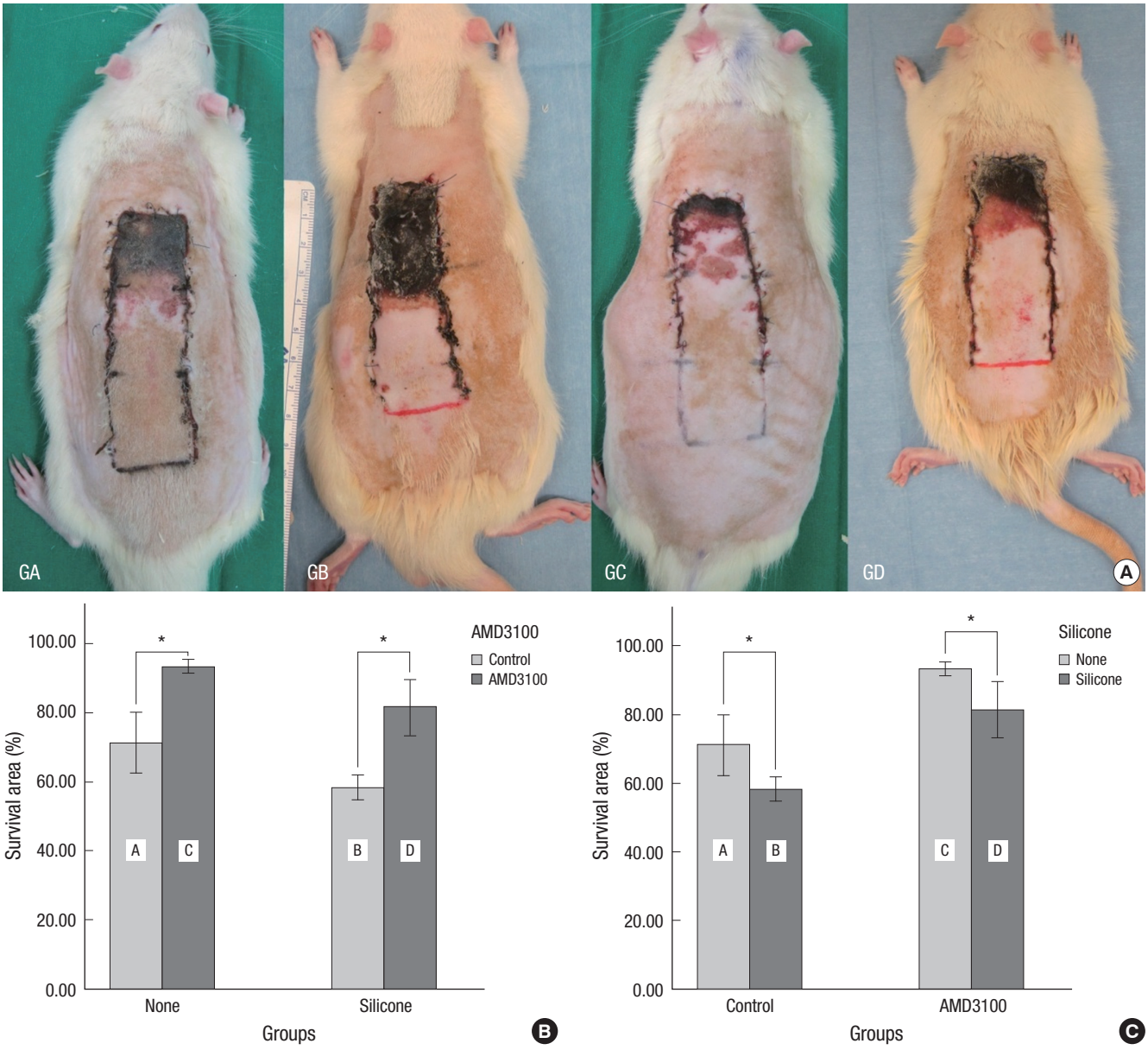

Fig. 2. Flap survival in the preliminary study of unexpanded flaps. (**A**) Gross findings of the skin flaps. GA, Group A, control without silicone sheet; GB, Group B, control with silicone sheet; GC, Group C, AMD-3100 injection without silicone sheet; GD, Group D, AMD-3100 injection with silicone sheet. (**B**) Treatment with AMD-3100 significantly increased survival rates in classical unexpanded flaps, with or without insertion of a silicone sheet. (**C**) Insertion of a silicone sheet under the flap blocked the blood supply from the bed. In a classical unexpanded flap, the mean survival rate of flaps without insertion of a silicone sheet was greater than those with a silicone sheet, regardless of treatment with AMD-3100 (*$P < 0.05$, Mann-Whitney test).

Table 4. Survival rate of flaps in the preliminary study of unexpanded flaps

Group	Median rate (%) (min-max)	*P* value
A (control)	69 (65.0-82.0)	
B	59 (53.0-64.0)	0.011*
C	94 (89.6-95.4)	< 0.001*
D	85 (71.0-95.3)	0.127
†A vs. C		0.004*
†B vs. D		0.002*
†C vs. D		0.017*

*$P < 0.05$, Mann-Whitney test between control and other groups; †Mann-Whitney test between groups. (A) Group A, control without silicone sheet; (B) Group B, control with silicone sheet; (C) Group C, AMD-3100 injection without silicone sheet; (D) Group D, AMD-3100 injection with silicone sheet.

Table 5. Survival rate of flaps in the main study

Group	Median rate (%) (min-max)	*P* value
Group I	59 (52.8-64.0)	
Group II	50 (53.0-64.0)	0.082
Group III	61 (56.0-74.0)	0.530
Group IV	51.5 (42.0-63.0)	0.127
†II vs. IV		0.573
†III vs. IV		0.029*
†No expansion(I and III) vs. Expansion (II and IV)		0.004*
†Control (I and II) vs. AMD-3100 (III and IV)		0.443

Mann-Whitney test between group I and other groups (II, III, and IV). *$P < 0.05$, Mann-Whitney test; †Mann-Whitney test between groups.

http://dx.doi.org/10.3346/jkms.2014.29.S3.S237

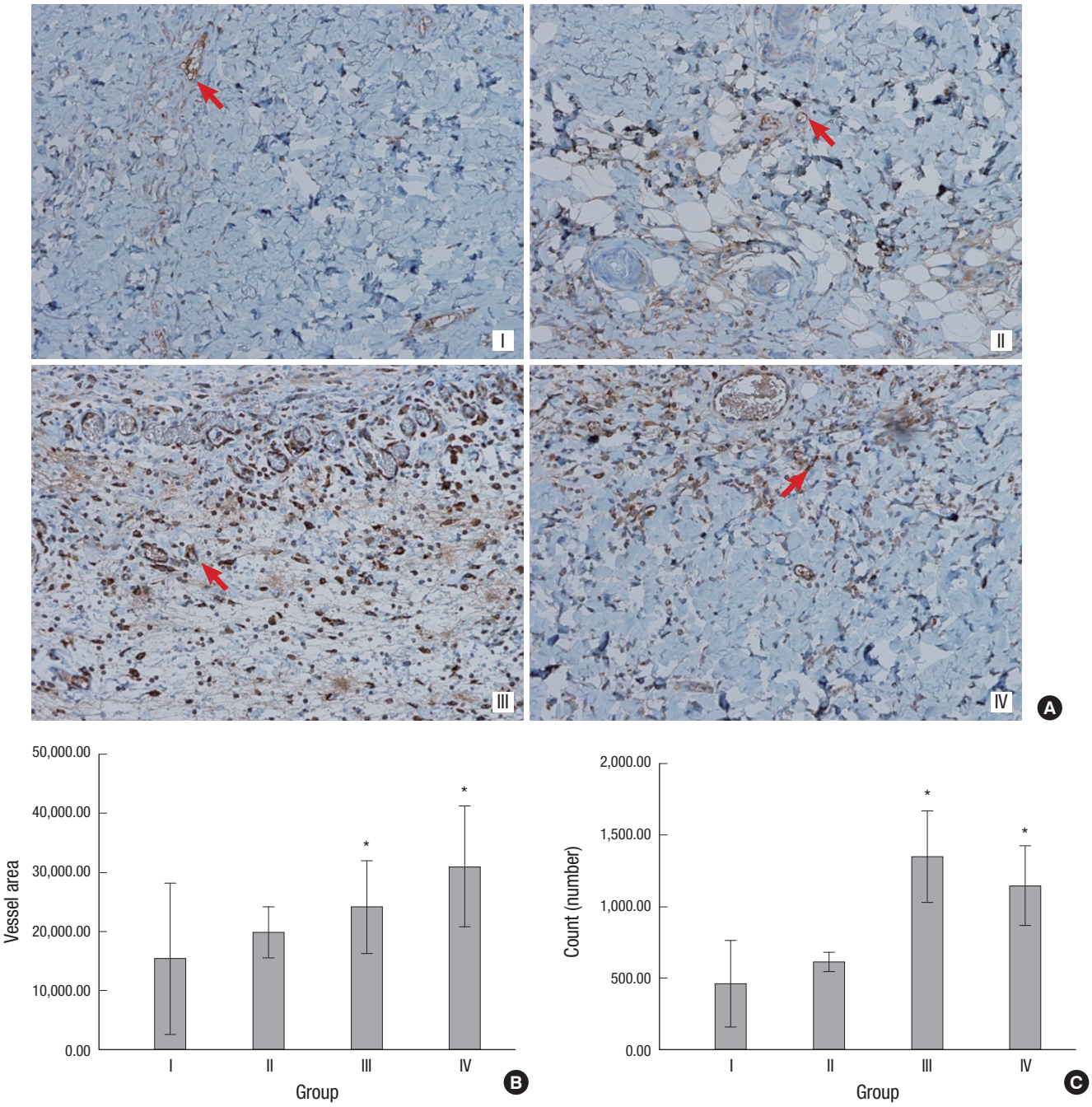

Fig. 3. Immunohistochemical staining for CD31 (**A**, 200×). Arrows indicate vessels. Vessel areas (**B**) and counts (**C**) by Group III and IV (received AMD-3100 injection) showed statistically significant increases in vessel number compared with group I (control) (*$P < 0.05$, Mann-Whitney test).

Real-time quantitative RT-PCR of VEGFA, VEGFR2, NOS3, SDF-1 and HIF-1α

RT-PCR was used to measure the change in levels of selected genes in the proximal portion of the flaps at postoperative day 7. The "fold change" in the gene for VEGFA was significantly increased in group II (1.5 ± 0.3, $P = 0.048$), group III (11.4 ± 12.6, $P = 0.024$) and group IV (11.4 ± 12.6, $P = 0.048$) compared to group I (control, Mann-Whitney test). The fold-change in the gene for VEGFR2 was significantly increased in group III (1.2 ± 0.3, $P = 0.024$) and group IV (1.31 ± 0.36, $P = 0.024$), but there was no change in the VEGFR2 gene in group II ($P = 0.167$) compared to group I (control, Mann-Whitney test). The expression of the gene for SDF-1 was significantly increased in group III (1.3 ± 0.6, $P = 0.024$), but there were no significant changes in the SDF-1 gene in group II or group IV ($P = 1.0$ and $P = 0.714$) compared to group I (control, Mann-Whitney test). The genes for NOS3 and HIF-1α were not significantly different between groups ($P = 0.903$, $P = 0.06$, Kruskal-Wallis test) (Fig. 5).

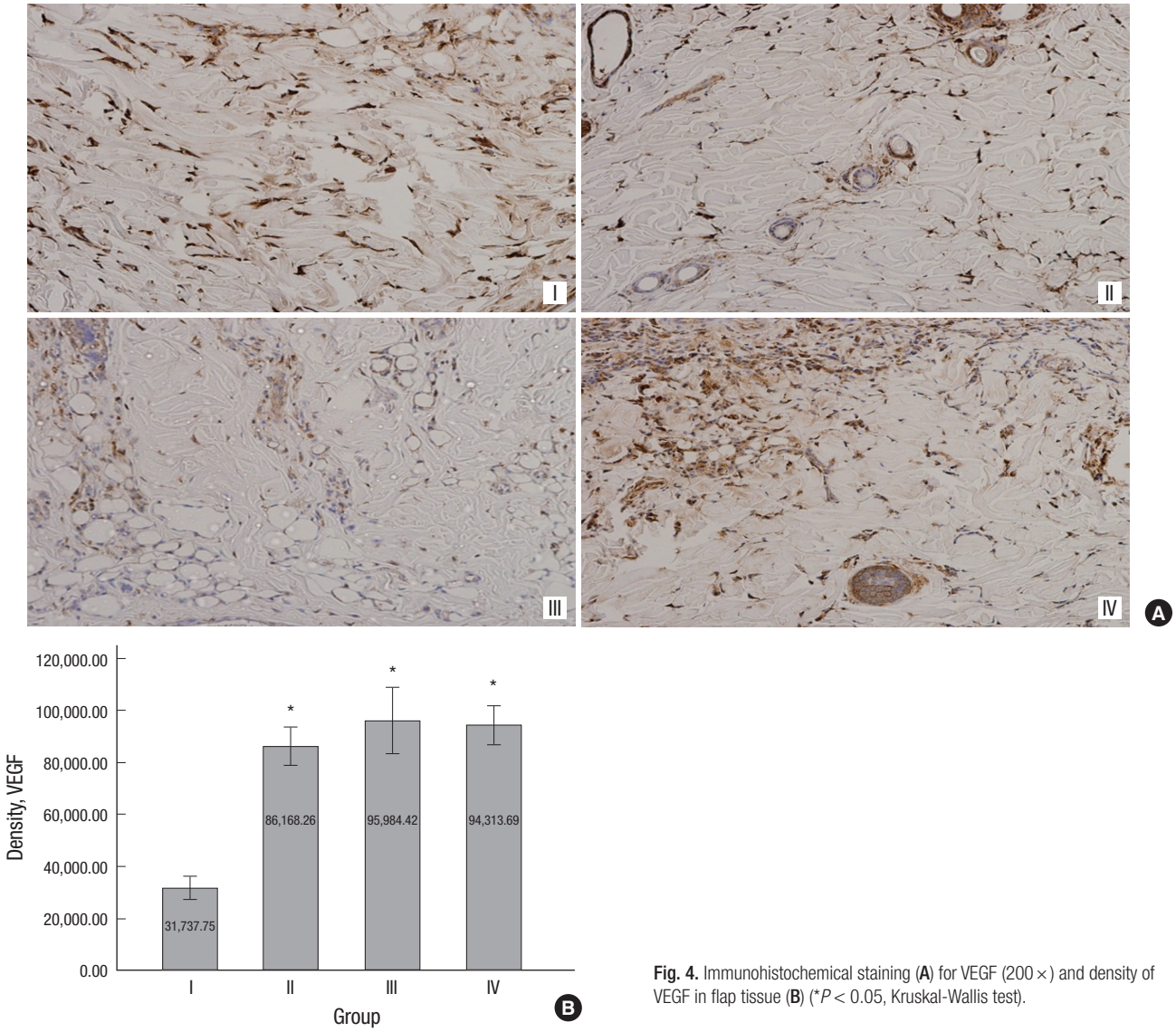

Fig. 4. Immunohistochemical staining (**A**) for VEGF (200×) and density of VEGF in flap tissue (**B**) (*$P < 0.05$, Kruskal-Wallis test).

DISCUSSION

Tissue flaps used for reconstruction of soft tissue defects must survive ischemic conditions by increasing vasculogenesis and angiogenesis at the flap itself and between the flap and the recipient site. For effective reconstruction using a tissue flap, the flap should have a larger survivable area with a smaller diameter pedicle, in order to reduce the morbidity of donor site. Gradual repeated tissue expansion at the donor site, which is going to be the flap, allows for greater neovascularization and regeneration of new skin by hypoxic and mechanical stimuli (17). This procedure has the advantage of expanding the survivable area of the donor flap despite the limited size of the donor tissue.

The most potent stimulus for neovascularization is hypoxia, which induces new blood vessel growth in order to restore adequate oxygen delivery to the ischemic tissue (12, 18). EPCs participate in neo-vascularization under ischemic conditions (19, 20). The ability of EPCs, but not mature endothelial cells, to proliferate in severely hypoxic conditions suggests a pivotal role for EPCs as the major building block for new vessels in ischemic tissues (21, 22). The gradient of hypoxia/ischemia ultimately directs EPCs to coalesce into independent vascular structures in order to restore tissue perfusion in the ischemic region (18). This gradient of hypoxia is established in both the classical caudally based dorsal skin flap and in the experimental expanded flap model (19). Tissue expansion, as in the expanded flap model, and vacuum assisted closure more effectively create the gradient of hypoxia surrounding the lesion during continuous expansion (23-25).

A disadvantage of the tissue expansion technique in large soft tissue defects, which require a long expansion time, is the inherent limit of the ability of the skin and soft tissue to regenerate (26). To address this concern, many methods have been reported to increase the efficacy of tissue expansion, such as in-

http://dx.doi.org/10.3346/jkms.2014.29.S3.S237

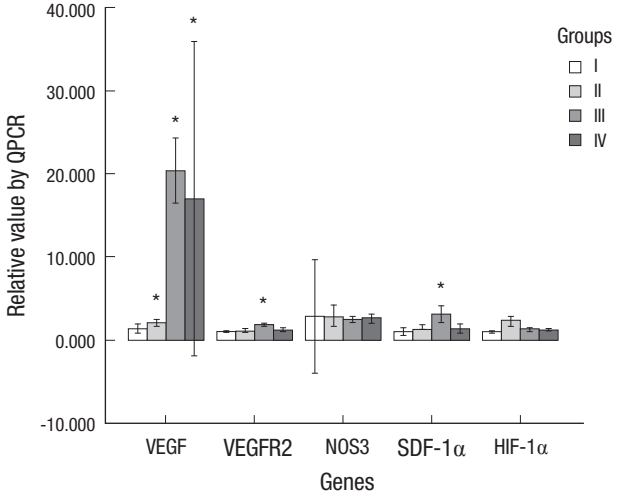

Fig. 5. Real time quantitative RT-PCR measurement of VEGFA, VEGFR2, NOS3, SDF-1 and HIF-1 (*$P < 0.05$, significant difference compared between control levels of group I by Mann-Whitney test).

traoperative acute skin stretching (27), transplanting bone marrow derived stem cells (26), and making use of compounds such as botulinum toxin (28), papaverine (29), dimethyl sulfoxide (30), and verapamil (31). Intermittent intraoperative skin stretching has been shown to improve flap viability by up-regulating VEGF and VEGFR2 at postoperative day 2 and decreasing necrosis by 50-75% at postoperative day 5 (27, 32). In order to increase the viability of tissue in expanded flaps and the efficacy of tissue expansion, it might be possible to enhance the recruitment of EPCs for vasculogenesis, increase VEGF concentration to induce angiogenesis, and create more favorable interactions with EPCs as a chemotactic factor.

Pretreatment of mice with G-CSF prior to administration of AMD-3100 has been shown to dramatically increase the mobilization of hematopoietic stem cells and neutrophils, but not EPCs, to the peripheral blood from the bone marrow. Pretreatment of mice with VEGF prior to administration of AMD-3100 has been shown to reduce the release of hematopoietic stem cells and leukocytes into the peripheral blood but to increase the mobilization of EPCs and mesenchymal stem cells (13, 15). Mobilization of EPCs is mediated by MMP-9 and regulated by hypoxic gradients through HIF-1α-inducted SDF-1 (CXCL12) in the bone marrow (7, 33). It has been reported that, immediately following a myocardial infarction (MI), acute antagonism of CXCR4 induced by AMD-3100 increases the number of EPCs in the peripheral blood for 1-2 weeks, improves survival and increases capillary density (34). AMD-3100-induced MMP-9 expression is mediated via VEGF (35). VEGFR2 increases as early as 2 hr after stretching and expression levels of these receptors return to the levels of non-stretched skin at day 7 (35).

In this study, the fraction of EPCs (VEGFR2+/CD34+ double positive cells) was highest in group IV (expanded flaps, treated with AMD-3100), which might have the most continuous ischemic conditions at postoperative day 2. The fraction of single positive VEGFR2+ cells in the peripheral blood in group III (not expanded, treated with AMD-3100) significantly increased at postoperative day 2. The expression levels of MMP-9 in the bone marrow and the fraction of EPCs in peripheral blood were both significantly increased the groups that received AMD-3100 (III and IV) in comparison with the groups that did not receive AMD-3100 (I and II). These results suggest that AMD-3100 contributes to the effective endogenous mobilization and differentiation of bone marrow derived hematopoietic stem cells to the peripheral blood in response to ischemic conditions of flaps by increasing VEGFR2-positive cells and EPCs (VEGFR2/CD34 double positive cells) in the peripheral blood. Furthermore, bone marrow derived stem cells might differentiate according to the level of ischemia of the flap in the presence of AMD-3100.

To investigate the condition of the microenvironment under expansion and AMD-3100, we harvested the proximal tissues of flaps and analyzed these tissues by immunohistochemistry, western blotting and real-time quantitative RT-PCR to detect VEGFA, VEGFR2, SDF-1, NOS-3, and HIF-1α.

The expression levels of VEGF in groups II, III and IV, as measured by immunohistochemistry (Fig. 3) and real-time quantitative RT-PCR (Fig. 5), were statistically significantly higher than in group I at postoperative day 7. These results suggest that AMD-3100 and tissue expansion may play a favorable role in increasing VEGF. SDF-1 and VEGFR2 in the classical unexpanded flap treated with AMD-3100 were expressed at statistically significantly higher levels than in group I (control,) as measured by real-time quantitative RT-PCR (Fig. 5). This might be correlated with the result of flow cytometry analysis showing that the fraction of VEGFR2 positive cells in the peripheral blood was higher than other group at postoperative day 2. VEGF and SDF-1 have been known to have direct and indirect effects on EPCs in a neovascularization system, including recruitment of EPCs from the bone marrow into the blood circulation by an MMP-9-dependent mechanism, homing and proliferation of EPCs, and incorporation into new vessels (34, 36). EPCs also mediate the release of VEGF and SDF-1 at the ischemic lesion, in a paracrine fashion (37).

NOS3 enzymatically generates nitric oxide (NO) in endothelial cells and regulates vascular functions such as smooth muscle relaxation and vasodilation. NOS3 may stimulate neovascularization due to VEGF, although enhancement of ischemia-induced angiogenesis by eNOS overexpression is not dependent on VEGF (38, 39). In our studies, there was no difference in the level of expression of HIF-1α and NOS3 between groups at postoperative day 7 (Fig. 5). This suggests that the severity of ischemia may be similar between the flaps, regardless of whether or not the flaps were expanded. VEGFA was highly expressed in group II, group III, and group IV though the constant expres-

sion level of NOS3 in different groups may not affect the vascular function or the neovascularization of the flaps.

Vessel area and the number of vessels in the proximal flaps at postoperative day 7 were increased in rats treated with AMD-3100 compared with flaps from untreated rats, regardless of whether or not the flaps were expanded (Fig. 3).

Although treatment with AMD-3100 increased neovascularization at ischemic flaps, it didn't affect the survival of ischemic flaps if there was a silicone sheet under the flap or the physiologic blood flow as measured by laser Doppler system. In some experiments, a thin silicone sheet was inserted under the classical dorsal skin flap in the rat model in order to permit the unidirectional caudally based blood flow. With the silicone sheets in place, the survival area of the flap was measured while blocking the vessel formation from the recipient bed. However, flaps with the same shape and pattern of blood flow (without inserting the silicone sheet) have similar survival areas to the general clinical situation. Therefore, the purpose of preliminary study was to evaluate the effect AMD-3100 while blocking the vasculogenesis and angiogenesis from the recipient. This preliminary study showed that antagonism of CXCR4 induced by AMD-3100 improved flap survival by 94% without the insertion of a silicone sheet. On the other hand, in rats treated with AMD-3100 and using the classical unexpanded dorsal skin flap with the adoption of a silicone sheet under the flap to allow only one-way blood perfusion from the proximal pedicle, flap survival decreased to 85% (Fig. 2). In the expanded flaps in mice treated with AMD-3100 the survival rate decreased further to 51.5% (Table 5). Although AMD-3100 increases the survival rate of flaps, insertion of a silicone sheet between the flap and the recipient along with tissue expansion might adversely affect the survival of flaps. Expansion may extend the survival area of the flap by increasing the ischemic conditions leading to greater induction of VEGF, but the area of new vessel formation blocked from the bed in expanded flap (5 × 10 cm), was larger than that of unexpanded flap (3 × 9 cm). Therefore, unexpanded flaps treated with AMD-3100 may have a statistically higher level of flap survival than the expanded flap with AMD-3100. Expanded flaps showed a decreased survival rate in comparison with unexpanded flaps, regardless of whether or not they were treated with AMD-3100. This phenomenon also adversely affected the survival of flaps, so that the survival rate of flaps was not statistically significantly different between groups.

In addition to the disadvantage of blocking the neovascularization between flap and recipient site with a silicone sheet, it was assumed that the survival rate in this main experiment may have been modulated by the systemic condition of the host rats and the requirement for the regeneration of other tissues. The size of our designed flap and silicone implant seemed large and the surgical time required to prepare the flaps was relatively long. Both the increased size of the flap and the increased surgical time are potentially fatal to the rats. Therefore, in these rats, bone marrow derived stem cells may be redirected to play roles in the recovery of organ functions (e.g. heart, liver, kidney), rather than participating in wound healing and tissue regeneration, especially in the expanded flap model.

Most reconstruction methods for soft tissue defects adopt various types of flaps permitting three-dimensional vascularization, with the exception of expanded flaps that use an internal tissue expander. These results suggest that AMD-3100 can effectively rescue the unstable viability of flap and ischemic tissue of recipient site, which is unexpectedly threatened by the wrong design of flap, trauma to pedicle and poor circulation around the flap. Furthermore, in surgery utilizing tissue expansion, only one incision is usually made to insert the tissue expander. Vascularization and tissue regeneration can be further increased by systemic mobilization of EPCs and mesenchymal stem cells in response to the ischemic conditions if the rat is treated with AMD-3100 during expansion.

In conclusion, treatment of AMD-3100 and tissue expansion may have the favorable role to increase VEGF levels in the tissue under ischemic conditions. AMD-3100 plays a role in the mobilization of endogenous EPCs and seems to increase vasculogenesis and angiogenesis in ischemic flaps, regardless of expansion. The EPCs have a paracrine effect on the induction of VEGF and SDF-1 at the ischemic area. However, this mobilization of endogenous EPCs may be affected by the vascularity surrounding the flap and that the vital condition of rats with the expanded flap model may cause burden to the hosts.

ACKNOWLEDGEMENTS

We acknowledge the major contribution of the clinical fellows of the Myongji Hospital and Severance Hospital: Hyung-Suk Kim, M.D., Yeon-Rum Jeon, M.D., Han-Su Yoo, M.D., Hyun-Joon Hong, M.D. We appreciate for kind support from Joo-Yeon Seok, a veterinarian of Department of Laboratory Animal Resources, Yonsei University College of Medicine. This paper has been presented at the 12th Korea-Japan Congress of Plastic and Reconstructive Surgery, held on May 15th, 2014, Incheon, Korea.

DISCOLOSURE

The authors have no potential conflicts of interest to disclose.

ORCID

Hii-Sun Jeong *http://orcid.org/0000-0001-9408-8207*

REFERENCES

1. Cho JY, Jang YC, Hur GY, Koh JH, Seo DK, Lee JW, Choi JK. *One stage*

 http://dx.doi.org/10.3346/jkms.2014.29.S3.S237

reconstruction of skull exposed by burn injury using a tissue expansion technique. Arch Plast Surg 2012; 39: 118-23.
2. Gur E, Zuker RM. *Complex facial nevi: a surgical algorithm. Plast Reconstr Surg 2000; 106: 25-35.*
3. Zuker RM, Filler RM, Lalla R. *Intra-abdominal tissue expansion: an adjunct in the separation of conjoined twins. J Pediatr Surg 1986; 21: 1198-200.*
4. Sasaki GH, Pang CY. *Pathophysiology of skin flaps raised on expanded pig skin. Plast Reconstr Surg 1984; 74: 59-67.*
5. Cherry GW, Austad E, Pasyk K, McClatchey K, Rohrich RJ. *Increased survival and vascularity of random-pattern skin flaps elevated in controlled, expanded skin. Plast Reconstr Surg 1983; 72: 680-7.*
6. Lantieri LA, Martin-Garcia N, Wechsler J, Mitrofanoff M, Raulo Y, Baruch JP. *Vascular endothelial growth factor expression in expanded tissue: a possible mechanism of angiogenesis in tissue expansion. Plast Reconstr Surg 1998; 101: 392-8.*
7. Ceradini DJ, Kulkarni AR, Callaghan MJ, Tepper OM, Bastidas N, Kleinman ME, Capla JM, Galiano RD, Levine JP, Gurtner GC. *Progenitor cell trafficking is regulated by hypoxic gradients through HIF-1 induction of SDF-1. Nat Med 2004; 10: 858-64.*
8. Takei T, Mills I, Arai K, Sumpio BE. *Molecular basis for tissue expansion: clinical implications for the surgeon. Plast Reconstr Surg 1998; 102: 247-58.*
9. Salibian AA, Widgerow AD, Abrouk M, Evans GR. *Stem cells in plastic surgery: a review of current clinical and translational applications. Arch Plast Surg 2013; 40: 666-75.*
10. Sung HM, Suh IS, Lee HB, Tak KS, Moon KM, Jung MS. *Case reports of adipose-derived stem cell therapy for nasal skin necrosis after filler injection. Arch Plast Surg 2012; 39: 51-4.*
11. Choi J, Minn KW, Chang H. *The efficacy and safety of platelet-rich plasma and adipose-derived stem cells: an update. Arch Plast Surg 2012; 39: 585-92.*
12. Isner JM, Asahara T. *Angiogenesis and vasculogenesis as therapeutic strategies for postnatal neovascularization. J Clin Invest 1999; 103: 1231-6.*
13. Kolonin MG, Simmons PJ. *Combinatorial stem cell mobilization. Nat Biotechnol 2009; 27: 252-3.*
14. Brave M, Farrell A, Ching Lin S, Ocheltree T, Pope Miksinski S, Lee SL, Saber H, Fourie J, Tornoe C, Booth B, et al. *FDA review summary: Mozobil in combination with granulocyte colony-stimulating factor to mobilize hematopoietic stem cells to the peripheral blood for collection and subsequent autologous transplantation. Oncology 2010; 78: 282-8.*
15. Pitchford SC, Furze RC, Jones CP, Wengner AM, Rankin SM. *Differential mobilization of subsets of progenitor cells from the bone marrow. Cell Stem Cell 2009; 4: 62-72.*
16. Pfaffl MW. *A new mathematical model for relative quantification in real-time RT-PCR. Nucleic Acids Res 2001; 29: e45.*
17. De Filippo RE, Atala A. *Stretch and growth: the molecular and physiologic influences of tissue expansion. Plast Reconstr Surg 2002; 109: 2450-62.*
18. Tepper OM, Capla JM, Galiano RD, Ceradini DJ, Callaghan MJ, Kleinman ME, Gurtner GC. *Adult vasculogenesis occurs through in situ recruitment, proliferation, and tubulization of circulating bone marrow-derived cells. Blood 2005; 105: 1068-77.*
19. Park S, Tepper OM, Galiano RD, Capla JM, Baharestani S, Kleinman ME, Pelo CR, Levine JP, Gurtner GC. *Selective recruitment of endothelial progenitor cells to ischemic tissues with increased neovascularization. Plast Reconstr Surg 2004; 113: 284-93.*
20. Zan T, Li Q, Dong J, Zheng S, Xie Y, Yu D, Zheng D, Gu B. *Transplanted endothelial progenitor cells increase neo-vascularisation of rat pre-fabricated flaps. J Plast Reconstr Aesthet Surg 2010; 63: 474-81.*
21. Asahara T, Kawamoto A, Masuda H. *Concise review: circulating endothelial progenitor cells for vascular medicine. Stem Cells 2011; 29: 1650-5.*
22. Takahashi T, Kalka C, Masuda H, Chen D, Silver M, Kearney M, Magner M, Isner JM, Asahara T. *Ischemia- and cytokine-induced mobilization of bone marrow-derived endothelial progenitor cells for neovascularization. Nat Med 1999; 5: 434-8.*
23. Borgquist O, Ingemansson R, Malmsjö M. *Wound edge microvascular blood flow during negative-pressure wound therapy: examining the effects of pressures from -10 to -175 mmHg. Plast Reconstr Surg 2010; 125: 502-9.*
24. Djedovic G, Kronberger P, Pierer G, Rieger UM. *Technical note on vacuum assisted closure-basket fixation of scrotal skin grafts. Arch Plast Surg 2013; 40: 641-2.*
25. Park CW, Kim YH, Hwang KT, Kim JT. *Reconstruction of a severely crushed leg with interpositional vessel grafts and latissimus dorsi flap. Arch Plast Surg 2012; 39: 417-21.*
26. Yang M, Li Q, Sheng L, Li H, Weng R, Zan T. *Bone marrow-derived mesenchymal stem cells transplantation accelerates tissue expansion by promoting skin regeneration during expansion. Ann Surg 2011; 253: 202-9.*
27. Shrader CD, Ressetar HG, Luo J, Cilento EV, Reilly FD. *Acute stretch promotes endothelial cell proliferation in wounded healing mouse skin. Arch Dermatol Res 2008; 300: 495-504.*
28. Chenwang D, Shiwei B, Dashan Y, Qiang L, Bin C, Muxin Z, Pengcheng L, Senkai L. *Application of botulinum toxin type A in myocutaneous flap expansion. Plast Reconstr Surg 2009; 124: 1450-7.*
29. Tang Y, Luan J, Zhang X. *Accelerating tissue expansion by application of topical papaverine cream. Plast Reconstr Surg 2004; 114: 1166-9.*
30. Vinnik CA, Jacob SW. *Dimethylsulfoxide (DMSO) for human single-stage intraoperative tissue expansion and circulatory enhancement. Aesthetic Plast Surg 1991; 15: 327-37.*
31. Copcu E, Sivrioglu N, Sisman N, Aktas A, Oztan Y. *Enhancement of tissue expansion by calcium channel blocker: a preliminary study. World J Surg Oncol 2003; 1: 19.*
32. Zhu X, Hall D, Ridenour G, Boo S, Jennings T, Hochberg J, Cilento E, Reilly FD. *A mouse model for studying rapid intraoperative methods of skin closure and wound healing. Med Sci Monit 2003; 9: Br109-15.*
33. De Falco E, Porcelli D, Torella AR, Straino S, Iachininoto MG, Orlandi A, Truffa S, Biglioli P, Napolitano M, Capogrossi MC, et al. *SDF-1 involvement in endothelial phenotype and ischemia-induced recruitment of bone marrow progenitor cells. Blood 2004; 104: 3472-82.*
34. Jujo K, Hamada H, Iwakura A, Thorne T, Sekiguchi H, Clarke T, Ito A, Misener S, Tanaka T, Klyachko E, et al. *CXCR4 blockade augments bone marrow progenitor cell recruitment to the neovasculature and reduces mortality after myocardial infarction. Proc Natl Acad Sci U S A 2010; 107: 11008-13.*
35. Erba P, Miele LF, Adini A, Ackermann M, Lamarche JM, Orgill BD, D'Amato RJ, Konerding MA, Mentzer SJ, Orgill DP. *A morphometric study of mechanotransductively induced dermal neovascularization. Plast Reconstr Surg 2011; 128: 288e-99e.*
36. Pompilio G, Capogrossi MC, Pesce M, Alamanni F, DiCampli C, Achilli F,

Germani A, Biglioli P. *Endothelial progenitor cells and cardiovascular homeostasis: clinical implications. Int J Cardiol 2009; 131: 156-67.*

37. Gnecchi M, Zhang Z, Ni A, Dzau VJ. *Paracrine mechanisms in adult stem cell signaling and therapy. Circ Res 2008; 103: 1204-19.*
38. Namba T, Koike H, Murakami K, Aoki M, Makino H, Hashiya N, Ogihara T, Kaneda Y, Kohno M, Morishita R. *Angiogenesis induced by endothelial nitric oxide synthase gene through vascular endothelial growth factor expression in a rat hindlimb ischemia model. Circulation 2003; 108: 2250-7.*
39. Amano K, Matsubara H, Iba O, Okigaki M, Fujiyama S, Imada T, Kojima H, Nozawa Y, Kawashima S, Yokoyama M, et al. *Enhancement of ischemia-induced angiogenesis by eNOS overexpression. Hypertension 2003; 41: 156-62.*

http://dx.doi.org/10.3346/jkms.2014.29.S3.S237